

Modeling The X-ray Timing Properties Of Cygnus X-1 As Caused By Waves Propagating In A Transition Disk

R. Misra

Dept. of Physics & Astronomy, Northwestern University, Evanston, Illinois - 60208, U.S.A

Received _____; accepted _____

ABSTRACT

We show that waves propagating in a transition disk can explain the short term temporal behavior of Cygnus X-1. In the transition disk model the spectrum is produced by saturated Comptonization within the inner region of the accretion disk where the temperature varies rapidly with radius. Recently, the spectrum from such a disk has been shown to fit the average broad band spectrum of this source better than that predicted by the soft-photon Comptonization model. Here, we consider a simple model where waves are propagating cylindrically symmetrically in the transition disk with a uniform propagation speed (c_p). We show that this model can qualitatively explain (a) the variation of the power spectral density (PSD) with energy, (b) the hard lags as a function of frequency and (c) the hard lags as a function of energy for various frequencies. Thus the transition disk model can explain the average spectrum and the short term temporal behavior of Cygnus X-1.

Subject headings: accretion disks—black hole physics—radiation mechanisms: thermal—relativity—stars: Cygnus X-1

1. Introduction

The X-ray emission of the well known Black Hole system Cygnus X-1 shows two long term spectral states. The system spends most of its time in the hard state where the spectrum can be approximated as an power-law with an exponential cutoff around 100 keV. The radiative mechanism generally invoked to explain this spectrum is unsaturated Comptonization of soft photons in a hot plasma. A model where the hot plasma is in the form of an corona on top of a cold accretion disk (Haardt & Maraschi 1993; Liang & Price 1977) has been ruled out by spectral modeling of the spectrum (Gierlinski et al. 1997; Nowak et al. 1999). The hot plasma could then be a hot inner accretion disk with the soft photons either arising from the cold outer disk (Shapiro, Lightman & Eardley 1976), from a pre-shock flow (Chakrabarti 1997) or from internally produced Synchrotron photons as in the ADAF model (Narayan 1996).

In the transition disk model (Misra & Melia 1996), the structure of the disk is obtained using the standard α -disk model of Shakura & Sunyaev (1973) without the assumption that the effective optical depth (τ_{eff}) is greater than unity. For high accretion rates ($> \sim 10^{18}$ g sec⁻¹), τ_{eff} turns out (self-consistently) to be less than unity for the innermost regions. The disk is then forced to cool by bremsstrahlung self Comptonization which causes the temperature to be much hotter than that obtained by assuming black body emission. The temperature rapidly increase with decreasing radius in this region. Since the Compton y-parameter is always greater than unity (although $\tau_{eff} < 1$) the local spectrum is a Wien peak. The sum over all Wien peak from the different radii (and corresponding different temperatures) gives rise to a power-law which matches the observed spectrum of Cygnus X-1 (Misra & Melia 1996). A similar model has been used to explain AGN spectra (Maraschi & Molendi 1990). Fitting broad-band (2 - 200 keV) spectrum of Cygnus X-1 revealed that the transition disk model fits the data better than a simple Comptonization

one (Misra et al. 1998; Misra, Chitnis & Melia 1998). In particular an ad hoc additional Wien peak ($kT \approx 50\text{keV}$) feature required in the Comptonization fit to the spectrum (Gierlinski et al. 1997) is not required for the transition disk model fit.

Another way to differentiate between these theoretical models is by studying the timing analysis of this source. Recently RXTE observed Cygnus X-1 and measured the power spectral density (PSD) for various energy bins, the time lags between energy bins as a function of frequency and energy and the coherence function (Nowak et al 1999a). These observations indicate that if the time lag is due to light travel time through the plasma, the size of the plasma has to be around $10^4 GM/c^2$ (Kazanas, Hua & Titarchuk 1997) and the seed photon source has to be isotropic (Nowak et al. 1999b). To avoid the energy problem associated with such a large plasma, Bottcher & Liang (1999), proposed a model where the variations are due to “blobs” of cool, dense matter which spiral inwards through the hot plasma. However, it is not clear whether these models agree even qualitatively with all the trends in the temporal behavior of Cygnus X-1 as observed by RXTE.

Nowak et al. 1999b showed that the time delays could be due to linear disturbances propagating through the plasma provided the speed of propagation is much smaller than c and photons of different energies are predominately produced in different regions. While such a scenario is not natural in the framework of a Comptonizing plasma, the transition disk meets the above requirements. In this letter, we show that waves propagating in a transition disk at least match qualitatively with most of the temporal observations.

2. Waves in the transition disk

A complete solution for the steady state disk structure in the framework of the transition disk model can be obtained using physical parameters which are the mass

accretion rate, the black hole mass and the the viscosity parameter α (Misra & Melia 1996). However, for simplicity and clarity Misra et al. 1997 used an empirical model to fit the average photon spectrum of Cygnus X-1. In the empirical model (which differs from the transition model only in the parameterization form) the temperature profile is assumed to be of the form:

$$kT \propto r^n J^m \text{ keV} , \quad (1)$$

where r is the radius and $J(r) = 1 - (r_i/r)^{1/2}$. r_i is the radius of the last stable orbit, taken to be $r_i = 3R_g$, with $R_g \equiv 2GM/c^2$. Here n and m are free parameters obtained by fitting the spectrum. The local radiative mechanism for such disks is saturated Comptonization (i.e. a Wien peak) since the local y parameter obtained is greater than unity (Misra et al. 1998). Since the gravitational power per unit area $F_g \propto R^{-3}J(R)$, the photon flux at earth can be written as (Misra et al. 1998)

$$f_E(E) = \int_{r_i}^{r_o} F(E, r) dr \propto E^2 \int_{r_i}^{r_o} (kT)^{-4} \exp(-E/kT) r^{-2} dr \quad , \quad (2)$$

where E is the energy of the photon and r_o is the radius to which the transition disk extends. Misra et al. (1998) fitted this empirical model and obtained the best fit temperature profile $T(r)$ with $n \approx -2.5$, $m \approx 1$ and the maximum temperature to be ≈ 70 keV. This profile is shown in figure 1.

The temporal behavior of the source is studied using the count rate as a function of time in a certain energy band. It is useful to define a response function (Nowak et al. 1999b) for a particular energy band

$$g(r) = \int_{E_1}^{E_2} F(E, r) A(E) dE \quad (3)$$

where E_2 and E_1 are the limits of the energy band and $A(E)$ is the energy dependent effective area of the detector. In this paper, we have used approximate values of $A(E)$ for the RXTE detector. The normalized $g(r)$ for some of the energy bands used in this paper

are shown in figure 1. The plot indicates where most of the photons contributing to the channel arise in the disk. We have assumed throughout this paper that the transition disk extends till $50r_s$.

Following Nowak et al. (1999b), for simplicity, we shall consider waves propagating cylindrically symmetrically in the disk with a uniform propagation speed (c_p). Further only waves moving toward a sink in the origin are considered. The sink at the origin is represented as $\rho_s(r, t) = \delta(r)\rho_s(t)$ in the wave equation. In this formalism the Fourier transform of the observed light curve in an energy channel ($s(t)$) becomes (Nowak et al. 1999b, Morse & Feshbach 1953)

$$S(f) = \frac{P_s(f)}{2\pi} \int_{r_i}^{r_o} g(r) G_f(2\pi f, r) dr \quad (4)$$

where $P_s(f)$ is the Fourier transform of $\rho_s(t)$ and G_f is the Fourier transform of the relevant two-dimensional Green's function. This is solved to be (Nowak et al. 1999b, Morse & Feshbach 1953)

$$G_f(2\pi f, r) = i\pi H_0^{(2)}(kr) , \quad (5)$$

where $k^2 \equiv (2\pi f/c_p)^2$ and $H_0^{(2)}$ is the second Hankel function of order zero.

Several assumptions have been made in the above derivation. First, the propagation speed (c_p) is assumed to be a constant. Second, the sink is assumed to be located at the origin instead of r_i and third the temperature profile ($T(r)$) is assumed not to respond to the wave propagations. These assumptions highlight the limitation of the analysis to compare with observations.

3. Results

In figure 2 (a), we show the predicted time lags versus frequency between various energy bands compared with the observed values taken from Nowak et al. (1999a). Here,

$c_p = 3000r_g/secs = 0.2c$ for a $10M_\odot$ Black Hole which is the only free parameter in this analysis. Only for those values of frequency where the coherence function is near unity is considered (i.e $f < 10$ Hz). Considering the simplifying assumptions made in this analysis the results do qualitatively match the observations while there are discrepancies at higher frequencies.

Crary et al. (1998) have used approximately 2000 days of data from the BATSE to estimate the time lag between 20-50 keV and 50 - 100 keV bands in the frequency range 0.01 to 0.2 Hz. In figure 2 (b) we show the predicted time lag for the corresponding energy bands. The slope of the curve is similar to the observations in this frequency range. However, the observed time lag is ≈ 2 higher than the predicted one. This could mean that the wave propagation speed is generally slightly smaller than $0.2c$.

In figure 3, we show the predicted time lags versus energy for three different frequencies. The data are obtained from Nowak et al. (1999a). The logarithmic dependence for low energies is obtained for this model. Moreover, the predicted slope of the curves decreases with frequency matching the observed trend. Again at high frequency (≈ 10) Hz there is significant deviation from the observations.

The PSD cannot be predicted in the framework of this simple model since the Fourier transform of the sink term ($P_s(f)$ in eqn (4)) is unknown. Using the observed PSD we obtain $P_s(f)$ and present the result in figure 4 (a). Figure 4(a) also shows the predicted PSD_w if $P_s(f)$ was constant (i.e. white noise). It should be noted that in this model there is no exponential cutoff in PSD_w below 100 Hz. It would have been difficult to explain the observed PSD if there had been such a cutoff. Even though, the observed PSD cannot be directly inferred, the model does make predictions for the ratio of PSD in various energy bands since this is independent of $P_s(f)$. In figure 4 (b) we show two calculated ratio as a function of frequency and compare it with the observed values. The ratios have been

renormalized to one at a frequency 1 Hz. For a wide range of frequency the ratios are close to unity which shows that the PSD is not sensitive to the energy band. One also finds that there is a remarkable correspondence of the calculated ratios with the observed values as a function of frequency and for different energy bands. Note that for frequencies greater than 10 Hz, the present analysis is not adequate because of the lack of coherence.

In the framework of this model a transition in the temporal behavior might take place when $kr_{12} \approx 1$ where r_{12} is the distance between the maxima of $g(r)$ for the two energy bands under consideration. This would occur at a frequency $f_{tr} \approx c_p/(2\pi r_{12}) \approx 477/r_{12} \approx 15$ Hz for $r_{12} \approx 30r_g$ (figure 1). It is tempting to associate f_{tr} with the observed frequency where the coherence function drops below unity. At higher frequencies than f_{tr} damping or non-linear effects may be dominant giving rise to this effect.

In summary, waves propagating in a transition disk can qualitatively explain most of the temporal properties of Cygnus X-1. In the analysis only one additional parameter to the steady state disk model is used to explain the temporal behavior of the system.

There are several observational features like the high frequency lag and the “shelves” in the lag versus frequency plot which is yet to be explained. The absence of such features maybe due to the simplifying assumptions (described in the end of section 2) used in this analysis. The transition disk models are generically radiation pressure dominated and hence are subject to secular and thermal instabilities (Misra & Melia 1996). However, these instabilities may be suppressed by non local effects like advection or convection. Fast moving radial waves as required in the above model may be produced in such a quasi-stable disk.

The author would like to thank Ron Taam for useful discussions.

REFERENCES

- Bottcher, M., & Liang, E. P., 1999, ApJ, **511**, L37 Bottcher & Liang 1999 511 L37
- Chakrabarti, S.K., 1997, ApJ, **484**, 313.
- Crary, D. J. et al., 1998, ApJ, **493**, L71.
- Gierlinski et al., 1997, MNRAS, **288**, 958.
- Haardt, F. & Maraschi, L., 1993, ApJ, **413**, 507.
- Kazanas D., Hua, X. M., & Titarchuk, L., 1997, ApJ, **480**, 280.
- Liang, E.P. & Price, R.H., 1977, ApJ, **218**, 247.
- Maraschi, L. & Molendi, S., 1990, ApJ, **353**, 452.
- Misra, R. & Melia, F., 1996, ApJ, **467**, 405.
- Misra, R. & Chitnis, V. R., Melia, F. & Rao, A.R. 1997, **487**, 388.
- Misra, R. & Chitnis, V. R. & Melia, F., 1998, **495**, 407.
- Morse, P.M. & Feshbach, H., 1953, Methods of Theoretical Physics, Part 1 (New York: McGraw-Hill Book Company, Inc.)
- Narayan, R. 1996, ApJ, **462**, 136.
- Nowak, M. A., et al., 1999a, ApJ, **510**, 874.
- Nowak, M. A., et al., 1999b, ApJ, **515**, 726.
- Shakura, N.I. & Sunyaev, R.A. 1973, *Astr. Ap.*, **24**, 337.
- Shapiro, S.L., Lightman A.P. & Eardley, D.M. 1976, ApJ, **204**, 187.

Fig. 1—Temperature as a function of radius (solid line). The response function ($g(r)$) for various energy bins (dotted lines). From left to right the energy bins correspond to (a) 14.1 - 45 keV, (b) 6.0 - 8.2 keV and (c) 0 - 3.9 keV.

Fig. 2 (a)— Time lags as a function of frequency between 0 - 3.9 keV and (from top to bottom) (a) 14.1 - 45 keV, (b) 8.2 - 14.1 keV (solid line) ,(c) 6.0 - 8.2 keV and (d) 3.9 - 6.0 keV. The dots are the observed time lags taken from Nowak et al. (1999a) between 0 - 3.9 keV and 8.2 - 14.1 keV.

Fig. 2 (b)—Time lags as a function of frequency between 20 - 50 keV and 50 - 100 keV (solid line). The dashed line is the best fit to the observed values in the frequency range 0.01 - 0.2 Hz (Crary et al. 1998).

Fig. 3—Time lag as a function of energy for three different frequencies. circles: 0.3 Hz, squares: 1 Hz and triangles: 10 Hz. Points with error bars are data taken from Nowak et al. (1999a) for the corresponding frequencies.

Fig. 4— Top:(a) The observed PSD for energy bin 0-3.9 keV (solid line). The inferred sink function $P_S(f)$ required to match the observed PSD (dashed line). The PSD if $P_S(f)$ was a constant (PSD_w) which corresponds to white noise (dotted line). Bottom (b): The ratio of the PSD. PSD_{soft} is for energy bin 0 - 3.9 keV. PSD_{hard} is for energy bins 14.1 - 45 keV and 6.0 - 8.2 keV. Solid lines are the computed values while dotted lines correspond to the observed ratios taken from Nowak et al. (1999a).

Figure 1

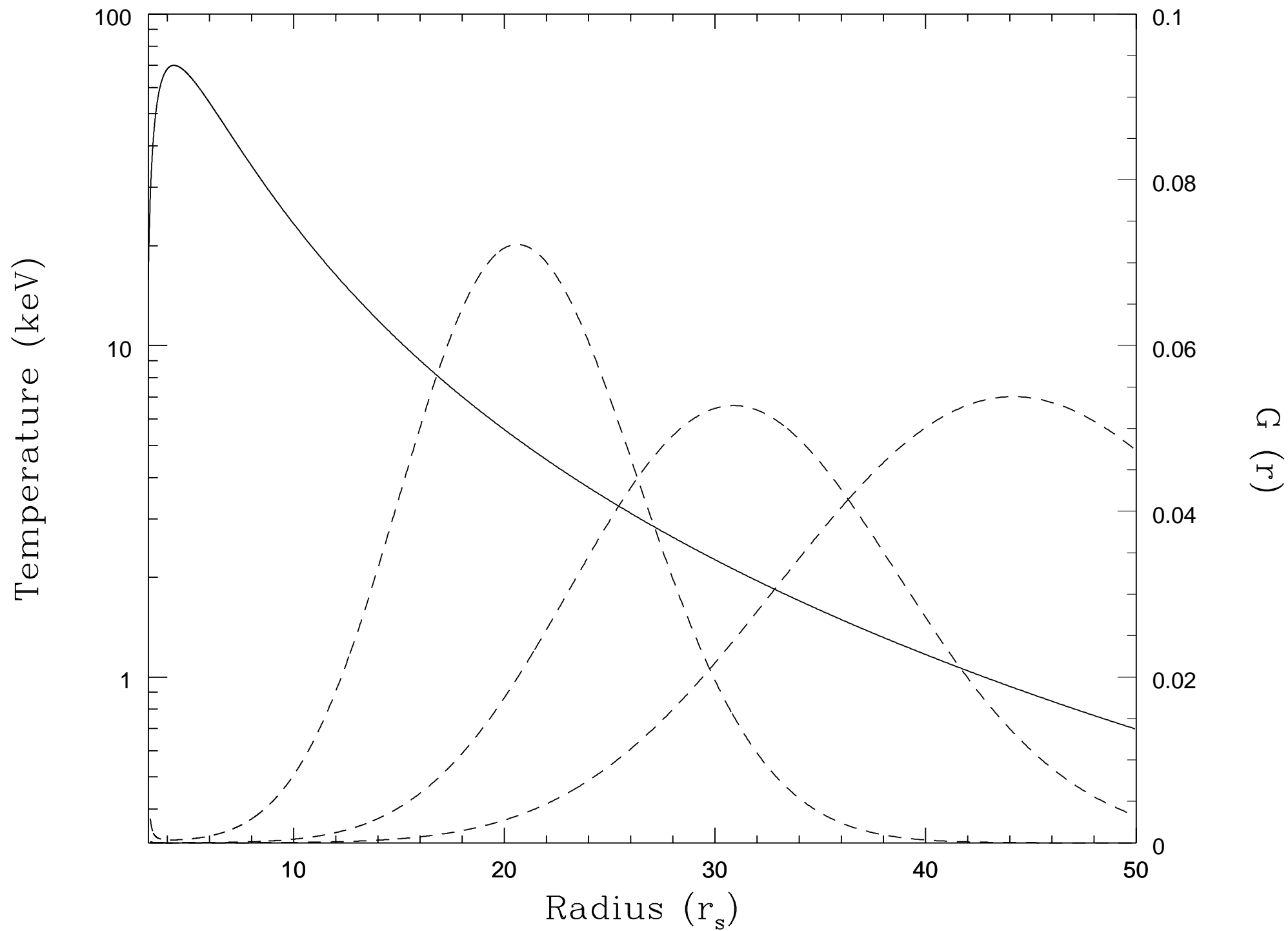


Figure 2 (a)

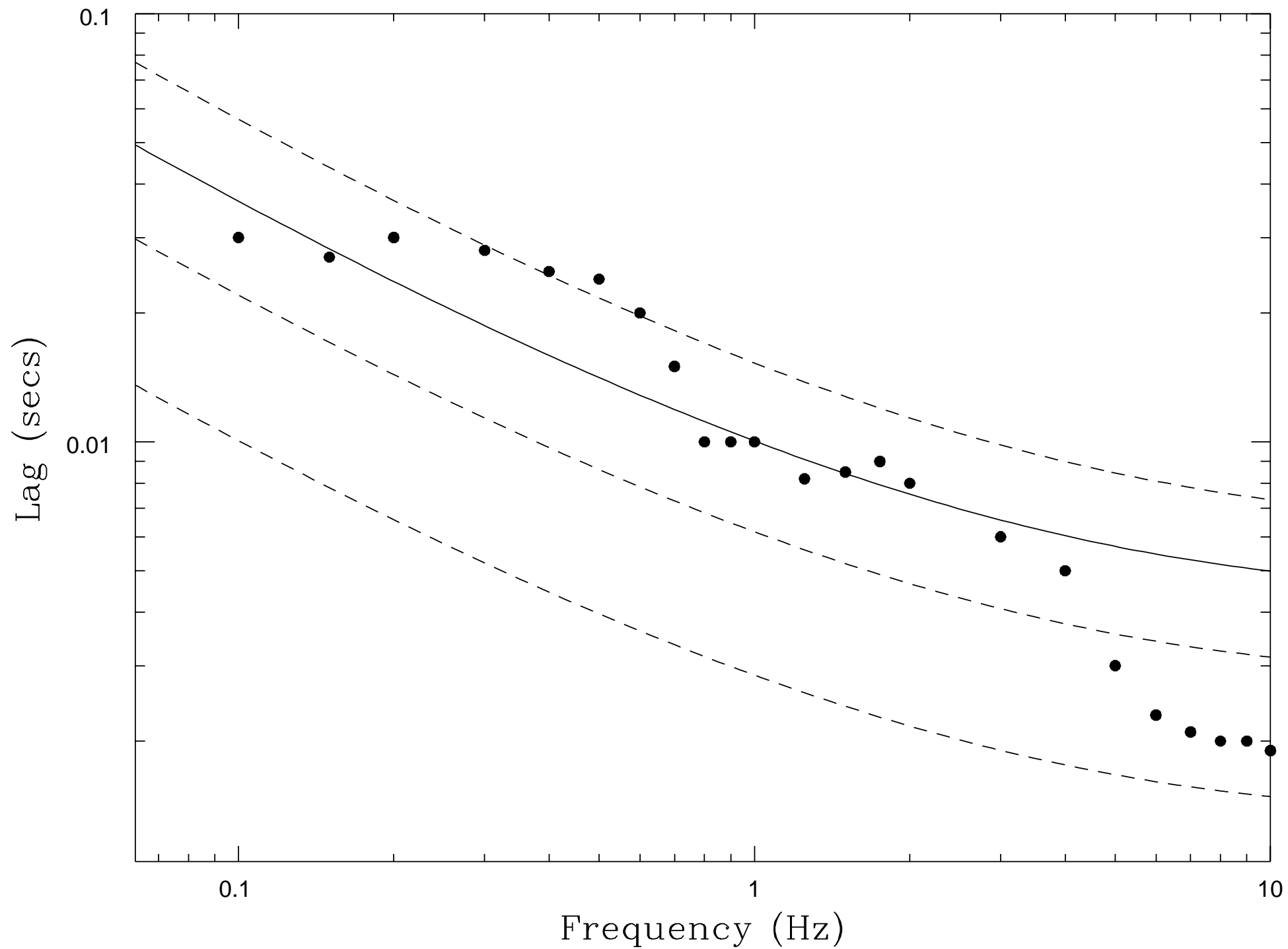


Figure 2 (b)

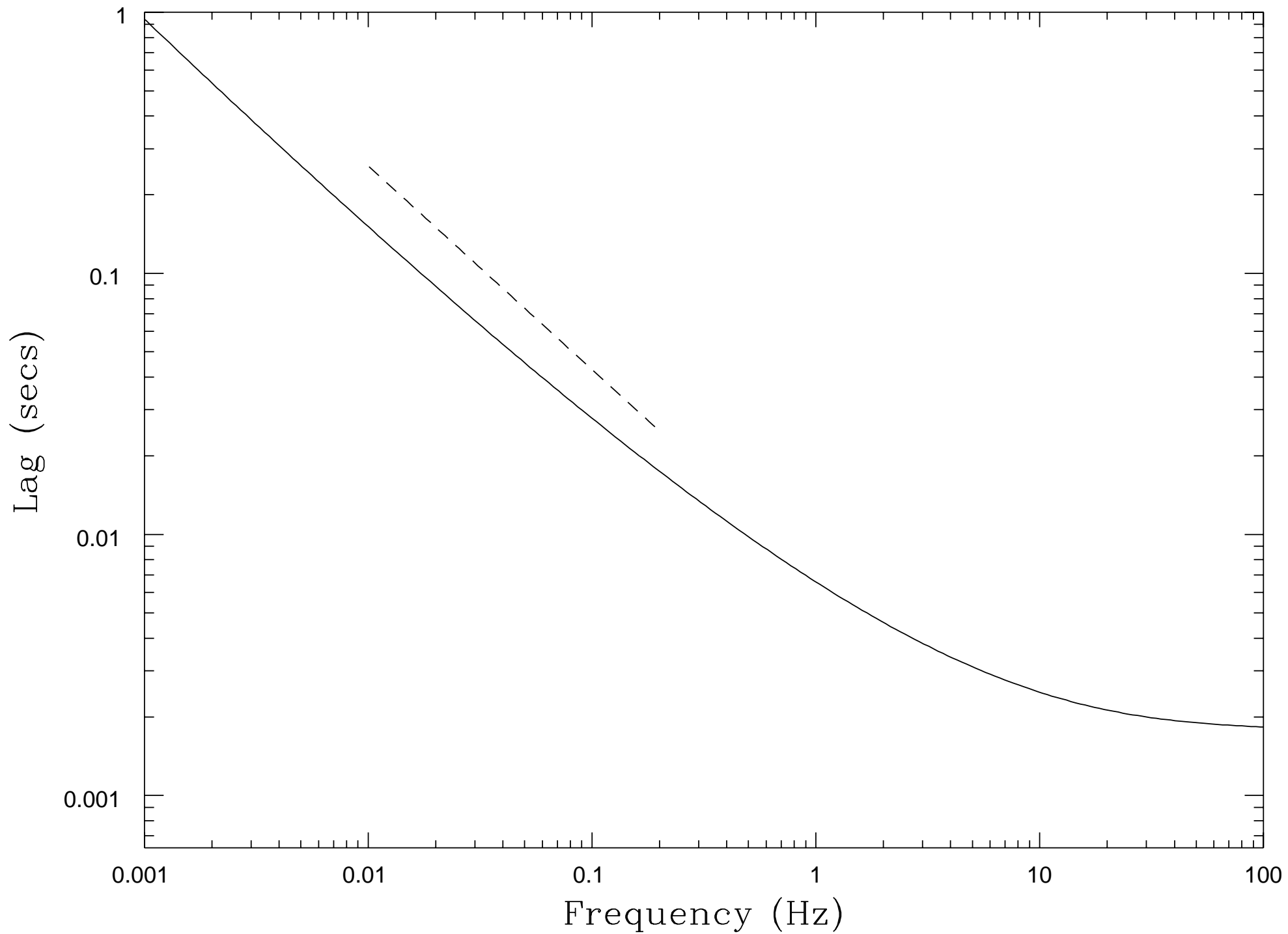


Figure 3

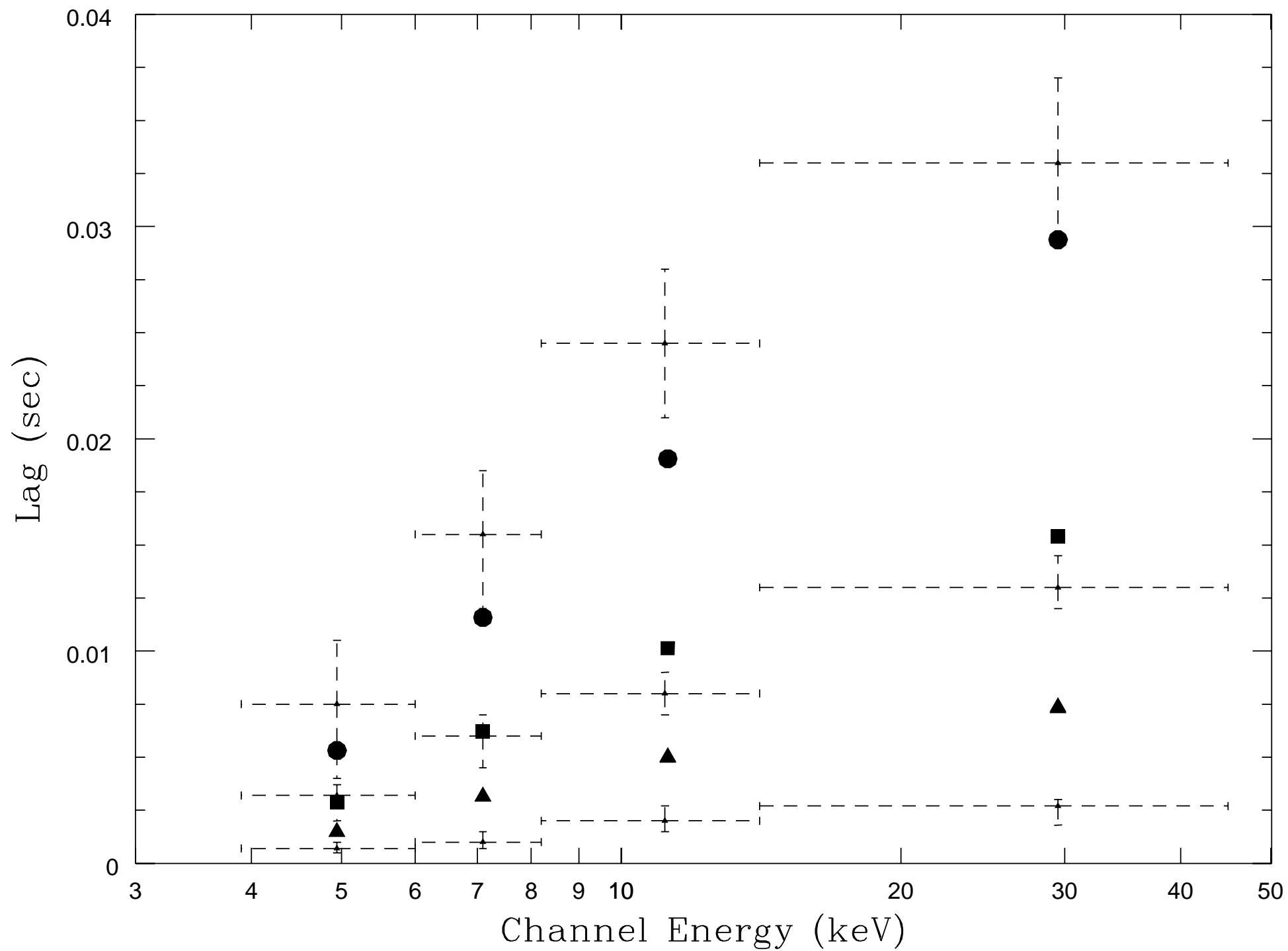


Figure 4

